

# From Infection to Detection: Imaging *S. aureus* – host interactions

U. Neugebauer<sup>1,2</sup>, C. Große<sup>1,2</sup>, M. Bauer<sup>1</sup>, B. Kemper<sup>3</sup>, A. Barroso-Pena<sup>3,5</sup>, A. Bauwens<sup>4</sup>, M. Glueder<sup>4</sup>, M. Woerdemann<sup>5</sup>, L. Dewenter<sup>5</sup>, C. Denz<sup>5</sup>, S. Kloß<sup>6</sup>, P. Rösch<sup>6</sup>, A. Sabat<sup>7</sup>, K. Schütze<sup>8</sup>, A. Friedrich<sup>7</sup>, G. von Bally<sup>3</sup>, J. Popp<sup>2,6</sup>, A. Mellmann<sup>4</sup>

<sup>1</sup> Center for Sepsis Control and Care, University Hospital Jena, Germany, ute.neugebauer@med.uni-jena.de

<sup>2</sup> Institute of Photonic Technology, Jena, Germany,

<sup>3</sup> Center for Biomedical Optics and Photonics, University of Münster, Münster, Germany,

<sup>4</sup> Institute for Hygiene, University of Münster, Münster, Germany,

<sup>5</sup> Institute of Applied Physics, University of Münster, Münster, Germany

<sup>6</sup> Institute of Physical Chemistry and Abbe School of Photonics, University Jena, Jena, Germany

<sup>7</sup> University Medical Centre Groningen, EurSafety Health-net, The Netherlands,

<sup>8</sup> CellTool GmbH, Tutzing, Germany

## Abstract

Infections, particularly those due to drug-resistant pathogens, significantly increase morbidity and mortality as well as cost of treatment and length of hospital stays. *Staphylococcus aureus*, a highly human-adapted organism, is the most common pathogen causing nosocomial infections. Among *S. aureus*, especially methicillin-resistant *S. aureus* (MRSA) causes problems in therapy and infection control. Understanding the mechanisms of infections is as important as the development of rapid tools for diagnosis. Within the Photonics4Life project “From Infection to Detection” these two goals are addressed. Modern optical technologies, such as multi-focus quantitative digital holographic microscopy (DHM) phase contrast, holographic optical tweezers (HOT) and Raman spectroscopy have been employed to analyse the cell morphology, cell dynamics and cellular refractive index of endothelial cells before and after incubation with *S. aureus* (or with model bacteria for HOT and DHM analysis). Individual bacteria inside the cells have been visualized and defined infection scenarios at the single cell level could be created. Finally, optical techniques were evaluated for further sub-typing of *S. aureus* strains and compared to the established *spa* typing method.

## 1 Introduction

*Staphylococcus aureus* is a highly human-adapted organism which can be found on the skin or nasal passage of around 20% of the human population without causing infections. However, under adequate conditions, such as a weakened immune system, *S. aureus* can use its elaborated infection mechanisms to enter the host cells and cause skin infections, or serious illnesses such as pneumonia, meningitis, osteomyelitis, endocarditis and even leading to sepsis. Nowadays, *S. aureus* is one of the most common pathogens causing nosocomial infections. If the bacteria carry antibiotic resistances they are especially hard to eliminate, significantly increase morbidity and mortality as well as cost of treatment and length of hospital stays. Among *S. aureus*, especially methicillin-resistant *S. aureus* (MRSA) causes problems in therapy and infection control. Figure 1 shows the prevalence of MRSA across Europe. In particular in the southern parts where antibiotics are frequently used, high prevalence of MRSA is recorded. Fast, reliable detection methods to prevent spreading of pathogens are needed as well as reliable tools for the prediction of colonization and pathogenic potential of *S. aureus* strains such as typing methods. Within the Photonics4Life (P4L) project “From Infection to Detection” an interdisciplinary team of clinicians, researchers and engineers from the optics and biophotonics background as well as two companies joined together to investigate the potential of novel biophotonic tools to study host-pathogen interactions. Understanding the mechanisms of infections might

enable the finding of new strategies for combating those infections. Furthermore, novel biophotonic (spectroscopic) approaches have been tested for their potential for fast *S. aureus* typing. The results are compared to the established *spa* typing methods where the sequence of the polymorphic X region of the protein A gene (*spa*) present in all strains of *S. aureus*<sup>1,2,3</sup> is used.

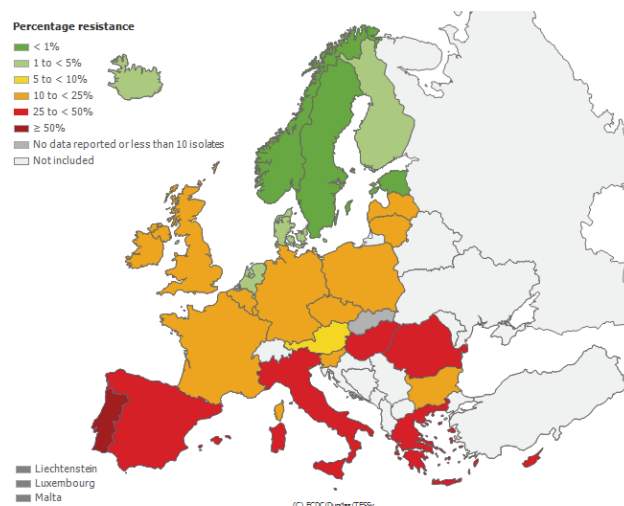


**Figure 1** Proportion of MRSA human blood isolates from participating countries in 2010. (Adapted from the European Antimicrobial Resistance Surveillance Network (EARS-Net)).

## 2 Methods

### 2.1 Cultivation of cells and bacteria

Cell-incubation experiments of EA.hy926 endothelial cells and human pancreatic ductal adenocarcinoma cells (PaTu8988T, DSMZ, Braunschweig, Germany) with *Staphylococcus aureus* (ATCC 6538) have been performed to investigate the mechanisms of host-pathogen-interaction. *Bacillus subtilis* (BD 630) have been used as model bacteria for the experiments with the holographic optical tweezers. EA.hy926 cells were grown in Dulbecco's Modified Eagle Medium (DMEM) supplemented with 10% fetal calf serum (FCS) at 37°C and 5% CO<sub>2</sub>. PaTu8988T were cultivated in DMEM with 5% FCS, 5% horse serum, and 2 mM L-glutamine at 10% CO<sub>2</sub>. *S. aureus* was cultivated in CASO-Bouillon at 37°C.

Sixteen different *S. aureus* strains belonging to four different *spa* groups have been collected at the University Medical Centre Groningen from human isolates and characterized using standard *spa* typing protocols.<sup>4</sup>

### 2.2 Holographic detection and manipulation

A recently described holographic workstation<sup>5,6</sup> was used to detect, track and manipulate pathogens and host cell in a label-free manner by digital holographic microscopy (DHM) and holographic optical tweezers (HOT)<sup>7</sup>. Briefly, a holographic optical tweezers system with a phase-only spatial light modulator (SLM) was combined with a digital holographic microscope (inverted Nikon Ti microscope with an extension module for Nomarsky differential interference contrast). One or multiple Gaussian shaped optical tweezers from a Nd:YVO<sub>4</sub> laser (Smart Laser Systems, Berlin, Germany,  $\lambda_{\text{HOT}} = 1064$  nm) with a maximal power at the sample plane of  $P_{\text{HOT}} = 250$  mW were used to manipulate the specimens. A frequency doubled Nd:YAG laser (Coherent, Compass 100, Lübeck, Germany,  $\lambda_{\text{DHM}} = 532$  nm) was used to generate quantitative phase images with DHM. A self-interference setup based on a Michelson interferometer<sup>8</sup> was adapted to one of the camera ports of the inverted microscope.

During the holographic measurements the pH was kept constant with HEPES buffer and the living cells were kept inside an incubation system with temperature control.

### 2.3 Raman spectroscopy

Raman spectroscopy is known to have high potential for the characterization<sup>9,10</sup> and differentiation<sup>11</sup> of bacteria. Furthermore, Raman spectroscopy was applied successfully to image biological cell<sup>12</sup>.

Infected and chemically fixed (4% formaline, 10 min) EA.hy926 endothelial cells in PBS were characterized by means of Raman spectroscopy using an upright micro-Raman setup (CRM 300, WITec GmbH, Germany). The exciting laser (532 nm, 15 mW at the sample) was focused through a 60x water immersion objective (Nikon, NA1.0).

Step size was 1  $\mu\text{m}$  for overview scans and 0.25  $\mu\text{m}$  for detailed scans with acquisition times of 0.5 s and 1 s per pixel, respectively.

Resonance Raman spectra of the different *S. aureus spa* types were excited at 244 nm (frequency doubled argon-ion laser, Innova 300, MotoFreD, Coherent Inc., Dieburg, Germany) and recorded with a micro-Raman setup (HR800, Horiba/Jobin-Yvon, Bensheim, Germany). Integration time for a single spectrum from bulk bacterial material was 60 s.

The BioRam instrument from the German company Cell-Tool was used to perform classification experiments between *S. aureus* and *Staphylococcus epidermidis*. The bacteria were embedded in hydrogel (Cellendes, Reutlingen) under physiological conditions (0.9% NaCl buffer, Braun) to allow easy access to microscopic observation while restricting the bacterial motility. The small layer of hydrogel allows Raman measurements at distance of the glass bottom minimizing the strong glass signal and enables relocating of the arrested bacteria at later time points.

## 3 Results

Modern optical technologies, such as multi-focus quantitative digital holographic microscopic (DHM) phase contrast, holographic optical tweezers (HOT) and Raman spectroscopy were applied to analyse the cell morphology, cell dynamics and cellular refractive index of endothelial cells before and after incubating with *S. aureus* for different infection periods. While DHM can follow the infection process in real time and investigate the dynamics of bacterial invasion and spreading inside the host cell as well as morphological changes of the host cell, Raman spectroscopy provides detailed, fingerprint-like chemical information of selected infection time points.

### 3.1 Holographic detection and manipulation

#### 3.1.1 Digital Holographic microscopy

Digital holographic microscopy (DHM) enables label-free, non-contact and non-destructive, quantitative and full-field phase contrast imaging of biological samples with a high spatial resolution. Fast single-shot acquisition of digital holograms can achieve a time resolution below 1 ms.

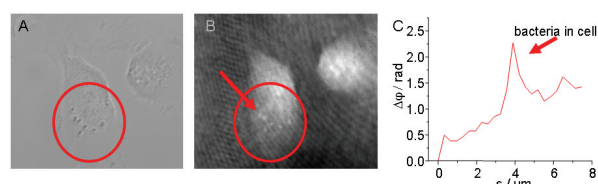


**Figure 2** *S. aureus* inside host cells are resolved in digital holographic microscopic (DHM) phase contrast. (A) White light image. (B) DHM phase contrast image. (C) Optical path length changes along a cross section in Figure B induced by the bacterial cells.

Figure 2B shows such a DHM quantitative phase image for a living EA.hy926 endothelial cell infected with *S. aureus*, in comparison with the corresponding white light image (Figure 2A). Darker, round spots are visible in the white light image which could be a hint for bacteria but could also be some cellular organelles. In the holographic phase contrast image the individual bacterial cells inside the host cell are resolved and identified based on the characteristic phase retardation. Figure 2C depicts a cross section through the image in Figure 2B and the local maximum indicates the phase retardation due to the bacteria. The localization of *S. aureus* inside the infected host cells was verified by Giemsa staining (not shown).

### 3.1.2 Manipulation with holographic optical tweezers (HOT)

In order to investigate the bacterial infection process it would be very advantageous to be able to arrange and position the pathogen and the host in the optimal configuration to create well-defined infection scenarios. This can be achieved by optical manipulation using HOT. In combination with the self-interference DHM module (see previous section 3.1.1), 3D object tracking with simultaneous cell morphology analysis by quantitative phase microscopy is possible.

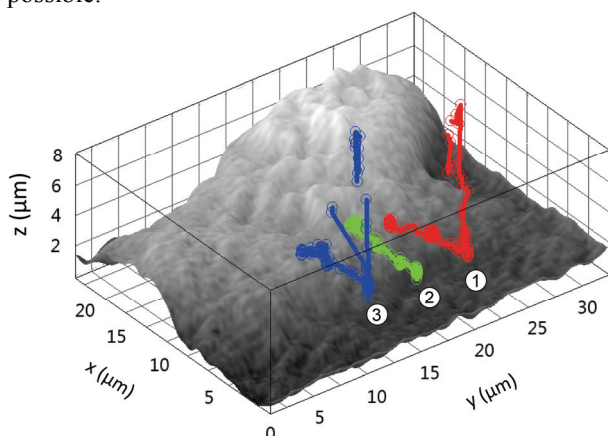


**Figure 3** 3D displacement trajectories of three bacterial cells superimposed to a gray level coded topography map of a living cell. (Adapted from Ref. <sup>5</sup>)

Figure 3 shows the topography map of an adherent PaTu8988T cell as obtained from a single digital hologram. To demonstrate the dynamic 3D positioning and tracking of holographic optical tweezers three *B. subtilis* cells were brought close to the cell and trapped there in the same *z*-plane. This starting point is symbolized with the numbered circles in Figure 3. Then, HOT were used to move the bacteria in *z* as well as in *x* and *y*-direction to approach them to the surface of the PaTu8988T cell. This was monitored by recording 110 digital holograms within 30 s. The respective displacement trajectories are depicted in Figure 3 in coloured lines. The morphology of the PaTu8988T cell did not change during optical manipulation of the bacteria indicating that no photodamage was induced by the HOT <sup>13</sup>.

## 3.2 Raman spectroscopic imaging

Following the same infection protocols as used for the digital holographic microscopy (section 3.1.1) samples were prepared for Raman spectroscopic imaging. Three hours after infection of the EA.hy926 endothelial cells with *S. aureus* the further infection process was stopped by chemically fixing the infected cells with paraformaldehyde. Raman spectroscopic imaging was performed in PBS buffer. Successfully, Raman spectroscopic images of *S. aureus* infected EA.hy926 cells and non-infected control cells could be recorded with a good signal-to-noise ratio. Overview scans of a whole cell with reduced spatial resolution (step size 1 μm) could be recorded in ca. 1 hour. Detailed Raman maps have been acquired with a reduced step size from the cellular region where bacteria were present inside the cell. With the help of statistical analysis methods such as vertex component analysis false colour Raman images have been created that clearly resolved the nucleus of the endothelial cell and individual *S. aureus* inside the cells. It was possible to identify single individual bacterial cells as well as very few small colonies composed of three to six bacteria. After the Raman experiments the cells were stained with Giemsa to proof the bacterial identification.

## 3.3 Staphylococcus subtyping

Typing of *S. aureus*, especially of MRSA, is an important measure to monitor the occurrence and spread of clones and to implement infection control measures. For *spa* typing the sequence of the polymorphic X region of the protein A gene is compared, which is ubiquitously present in *S. aureus*. Although *spa* typing is relatively cheap in comparison to classical methods such as pulsed-field gel electrophoresis (PFGE), it still takes 24-48 hours till the result. Therefore, novel biophotonic techniques, such as Raman spectroscopy have been tested for their potential to differentiate the different *S. aureus* subtypes. Only 60 s are needed to record a Raman spectrum from the bacteria.

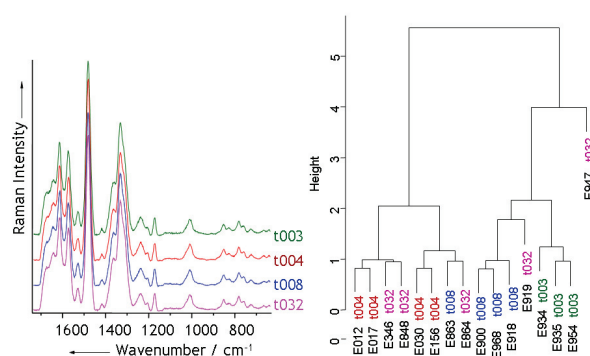


**Figure 4** (A) Averaged Raman spectra of four different *S. aureus spa* types excited at 244 nm. From each *spa* type three to five different strains have been included in the analysis. (B) Hierarchical cluster analysis of the averaged Raman spectra of the 16 different *S. aureus* strains. Labels show the strain name and (in color) the corresponding *spa* type.

Sixteen different *S. aureus* strains belonging to four different *spa* groups from human isolates have been collected at the University Medical Centre Groningen, Netherlands. UV resonance Raman spectra excited at 244 nm of those 16 strains have been recorded. The averaged Raman spectra for the four *spa* types are depicted in Figure 4A. Hierarchical cluster analysis of the averaged strain spectra yields a good separation between the individual strain types (Figure 4B). All three strains of the *spa* type t003 form one cluster and three out of four isolates of *spa* type t008 are grouped together which reflects the good agreement of *spa* typing and spectroscopy. However, for the isolates belonging to *spa* type t032 it was not possible to achieve a homogenous cluster based on the Raman data.

### 3.4 Development of Raman spectroscopic devices for bacteria analysis

The company CellTool was extending the application range of their BioRam for the non-contact and marker-free identification and differentiation of different bacterial strains from the genus *Staphylococci*. Raman spectra excited at 785 nm (80mW) have been recorded from *S. aureus* and *S. epidermidis*. The resulting Raman spectra showed clear spectral differences, especially in the higher content of carotenoids in *S. aureus*. Applying unsupervised principal component analysis (PCA) yielded two very well separated clusters (Figure 5) indicating the high potential of even further sub-classification.

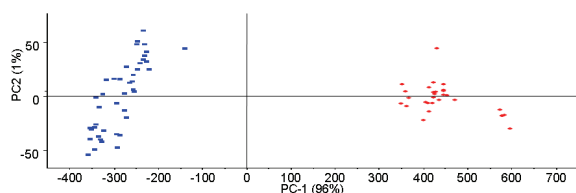


**Figure 5** 2D Score plot of the first two principal components showing good separation of *S. aureus* (blue squares) and *S. epidermidis* (red diamonds) along the first principal component (PC1).

## 4 Conclusions and Outlook

Optical technologies can provide a deeper insight into infections at the cellular level, such as following the infection process in real time with DHM or obtaining detailed chemical information with Raman spectroscopy for a specific infection time point.

Further experiments might enable the detection of differences in the host-pathogen interaction due to differences in pathogens of the same species comprising for example different pathogenicity factors or different alleles. When HOT, DHM and Raman are finally combined in one device a rapid tool for the prediction of colonization and pathogenic potential of *S. aureus* strains would be available for evaluation in the hospital setting and ultimately help to improve diagnosis and lead to a more suitable therapy.

## 5 Acknowledgement

Financial support from the EU within the “Framework Programme 7” for the Project “Photonics4Life (P4L grant agreement no.: 224014), from the Federal Ministry of Education and Research (BMBF), Germany via the integrated research and treatment center “Center for Sepsis Control and Care” (FKZ 534 01EO1002) and by the focus program “Biophotonics” (FKZ 13N10937) is highly acknowledged.

We thank Prof. Regine Heller for providing the EA.hy926 cell lines for the Raman experiments.

## 6 References

- (1) Harmsen, D.; Claus, H.; Witte, W.; Rothganger, J.; Turnwald, D.; Vogel, U. *Journal of Clinical Microbiology* **2003**, *41*, 5442-5448.
- (2) Strommenger, B.; Bräulke, C.; Heuck, D.; Schmidt, C.; Pasemann, B.; Nubel, U.; Witte, W. *Journal of Clinical Microbiology* **2008**, *46*, 574-581.
- (3) Hallin, M.; Friedrich, A. W.; Struelens, M. J. In *Molecular Epidemiology of Microorganisms* 2009; Vol. 551, p 189-202.
- (4) Mellmann, A.; Friedrich, A. W.; Rosenkötter, N.; Rothganger, J.; Karch, H.; Reintjes, R.; Harmsen, D. *Plos Medicine* **2006**, *3*, 348-355.
- (5) Kemper, B.; Barroso, A.; Woerdemann, M.; Dewenter, L.; Vollmer, A.; Schubert, R.; Mellmann, A.; von Bally, G.; Denz, C. *J. Biophotonics* **2012**, DOI 10.1002/jbio.201200057.
- (6) Esseling, M.; Kemper, B.; Antkowiak, M.; Stevenson, D. J.; Chaudet, L.; Neil, M. A. A.; French, P. W.; von Bally, G.; Dholakia, K.; Denz, C. *Journal of Biophotonics* **2012**, *5*, 9-13.
- (7) Woerdemann, M.; Alpmann, C.; Denz, C. In *Optical Imaging and Metrology*; Osten, W. R., N., Ed.; Wiley-VCH Verlag: Weinheim, 2012.
- (8) Kemper, B.; Vollmer, A.; Rommel, C. E.; Schneckeburger, J.; von Bally, G. *Journal of Biomedical Optics* **2011**, *16*.
- (9) Neugebauer, U.; Schmid, U.; Baumann, K.; Holzgrabe, U.; Ziebuhr, W.; Kozitskaya, S.; Kiefer, W.; Schmitt, M.; Popp, J. *Biopolymers* **2006**, *82*, 306-311.
- (10) Neugebauer, U.; Schmid, U.; Baumann, K.; Ziebuhr, W.; Kozitskaya, S.; Deckert, V.; Schmitt, M.; Popp, J. *ChemPhysChem* **2007**, *8*, 124-137.
- (11) Harz, M.; Rösch, P.; Popp, J. *Cytometry Part A* **2009**, *75A*, 104-113.
- (12) Krafft, C.; Neugebauer, U.; Popp, J. In *Vibrational Spectroscopic Imaging for Biomedical Applications*; Srinivasan, G., Ed.; McGrawHill: 2010.
- (13) Barroso Pena, A.; Kemper, B.; Woerdemann, M.; Vollmer, A.; Ketelhut, S.; von Bally, G.; Denz, C. *Proc. SPIE* **2012**, *8427*, 84270A-1.